LUONG TEST TO EVALUATE RESIDUAL SHEAR BEHAVIOR OF FRC

C. Aire[1], A. Blanco[2], P. Pujadas[3] and S. H. P. Cavalaro[4]

[1]PhD, Research Engineer, Instituto de Ingeniería – Ingeniería Estructural. Universidad Nacional Autónoma de México. Building 3-217. Circuito Escolar. Ciudad Universitaria, 04510 Mexico City (Mexico), aire@pumas.iingen.unam.mx
[2]PhD, Postodoctoral researcher, Dept. of Civil and Environmental Engineering, Universitat Politècnica de Catalunya-BarcelonaTech, Jordi Girona 1-3, Building C1-202, 08034 Barcelona (Spain), ana.blanco@upc.edu
[3]PhD, Postodoctoral researcher, Dept. of Civil and Environmental Engineering, Universitat Politècnica de Catalunya-BarcelonaTech, Jordi Girona 1-3, Building C1-202, 08034 Barcelona, (Spain), pablo.pujadas@upc.edu
[4]PhD, Associate Professor, Dept. of Civil and Environmental Engineering, Universitat Politècnica de Catalunya-BarcelonaTech, Jordi Girona 1-3, Building B1-106, 08034 Barcelona, (Spain), sergio.pialarissi@upc.edu

ABSTRACT

The behavior of concrete subjected to shear is a complex phenomenon; difficult to be evaluated experimentally. The characterization of the behavior of fiber reinforced concrete (FRC) under shear is even more complex since high displacements are required to assess the post-cracking residual shear response. Such high displacements might produce a change in the test setup, thus inducing bending moments that compromise the reliability of the results. The Luong test - originally proposed to assess shear in plain concrete and rocks - might be a suitable testing method for this purpose. However, no application of this test to FRC is found in the literature. The objective of this study is to propose a simple shear test and adapt it for FRC. For that, an experimental program of Luong test was performed on FRC mixes including steel and macro-synthetic fibers in different contents. Moreover, two variables related to the test setup were analyzed: the height of the specimen and the diameter of the circumferential notch. The results indicate that the Luong test meets the requirements to be applied to the characterization of the shear residual response of FRC in terms of sensitivity of the test and reliability.

Keywords: Shear, Luong test, Fiber reinforced concrete, FRC, Residual behavior, Characterization

Carlos Aire, PhD, Research Engineer
Universidad Nacional Autónoma de México
Circuito Escolar, Ciudad Universitaria
Mexico City, 04510
Mexico

Email: aire@pumas.iingen.unam.mx
Tel: +52 (55) 56233600

1. INTRODUCTION

Shear behavior in concrete can be significantly improved by the addition of fibers due to their contribution to the post-cracking residual strength and ductility [1]. As a result, in some cases the fibers may partially or totally substitute the stirrups [2,3]. Therefore, several design recommendations include formulations to take into account the contribution of the fibers to shear, which in general is evaluated through bending tests instead of shear tests [4-9]. Although a bending test is convenient to obtain the tensile constitutive curve for the design of FRC beams subjected to flexion, its use for the shear design may be considered questionable since the stress distribution and the contribution mechanism of the fibers in a crack due to bending may differ considerably from the observed in a crack due to shear.

Despite the link between the shear and the flexural behaviors, this might be a too rough approximation of reality with possible negative repercussion in terms of structural safety or optimization of material consumption. Likewise, the use of the bending test for the indirect quality control of the shear behavior is also questionable, especially in a material whose response is strongly dependent of fiber distribution. This situation arises partly due to the lack of a standard and a simple test method for the characterization or the quality control of shear in FRC. In fact, the complexity involved in most shear tests hinders their use for the systematic characterization of shear in the quality control of worksites.

Most of the shear tests found in the literature present an eccentricity in the loading, which can lead to a combination of a shear and bending failure. In addition, the majority also presents a setup that is not compatible with the requirements for FRC. Notice that in order to measure the contribution of the fibers in the shear post-cracking response, the setup should allow high values of displacement. This situation also leads to a higher influence of the bending in the failure mechanism of FRC shear tests since the bending forces during the test increase as the crack opens.

The most common shear test used to characterize FRC is the push-off test [10-14]. However, due to the test setup, the specimen may rotate during the loading. Even in the case of using a steel frame to confine the specimen, the accuracy of the measurements of the crack opening may be compromised as shown in [14]. In this context, it may be interesting to seek alternative setups for the shear characterization of FRC.

Taking this into account, the objective of the present study is to propose a test for the characterization of the direct shear response of FRC. An adaptation of the Luong test [15], which was originally conceived to evaluate shear in concrete and rocks, is adapted for the case of FRC. The main reason is that this test exhibits a failure mechanism that may allow high displacements without increasing noticeably the bending moment. For that reason, an experimental program of Luong tests on four FRC mixes was performed. Several variables regarding the test setup and the materials were evaluated, namely the height of the specimen, the diameter of the notch in the specimen, the type of fiber (one steel fiber and one macro-synthetic fiber) and the fiber content.

2. LUONG TEST

The Luong test is a shear test proposed by Luong [15] to evaluate direct shear in plain concrete and rocks. The test is performed in cylindrical specimen with circumferential concentric notches at the top and bottom surfaces (see Figure 1a). In the original setup the load is distributed in the entire inner and outer surface of the specimen, as shown in Figure 1a, which might induce additional eccentricity. For that reason, in the present study a metallic ring is put in contact with the outer perimeter of the notch at the top surface, whereas similar ring with smaller diameter is placed in contact with the inner part of the notch. The load is applied to the opposite surface of both rings in the form of a constant displacement rate (0.1 mm/min). This induces a shear loading of the concrete at the zone of the notch.

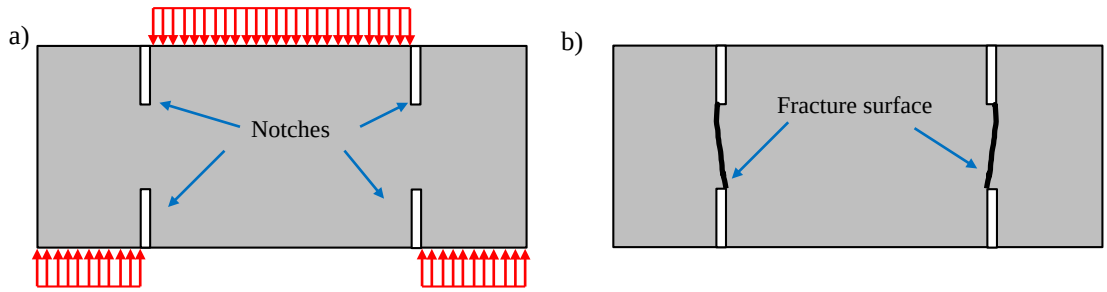

Figure 1. a) Original Luong test setup and b) ideal shear failure in the Luong test.

The failure mechanism is characterized by a crack along the plane of the notch when the shear strength of concrete is reached. As a result, a cylinder is formed in the internal area of the notch. Notice that for an ideal shear failure to occur, the fracture surface should be as vertical as possible (see Figure 1b). At this point, the main mechanism governing the shear behavior in plain concrete is the aggregate interlock. However, for FRC specimens the combination of the aggregate interlock and the fibers determines the shear behavior. As the stresses generated by the application of load increase, radial cracks appear in the external concrete crown.

3. EXPERIMENTAL PROGRAM

3.1. Materials and concrete mix

The experimental program involved the manufacturing of four FRC mixes. One steel fiber (SF) and one of macro-synthetic or plastic fiber (PF) were used in two different contents. In order to avoid introducing more variables to the study, the same concrete mix was considered in all cases with a water/cement ratio (w/c) of 0.5, a maximum aggregate size of 9.5 mm and a sand fineness modulus of 3.1. The cement employed in the mix was a Portland cement type CEM II. A water-reducing admixture was included in the mix to improve workability avoiding possible segregation. The details of the mixes are presented in Table 1. The SF used in mixes M1 and M2 presents hooked-ends and is glued into bundles. The macro-synthetic fiber PFA added in mixes M3 and M4 is a 100% virgin polypropylene fiber. The characteristics of the fibers are shown in Table 2.

Table 1. Concrete mixes.

Component	**Content**			
	M1	**M2**	**M3**	**M4**
Cement (kg/m^3)	428	428	428	428
Gravel (kg/m^3)	885	885	885	885
Sand (kg/m^3)	662	662	662	662
Water (kg/m^3)	214	214	214	214
Admixture (ml/m^3)	2000	2000	2000	2000
Fiber (kg/m^3)	40	60	5	7
Notation	**SF40**	**SF60**	**PF5**	**PF7**

Table 2. Characteristics of the fibers.

Characteristics	**SF**	**PF**
Length (mm)	35	54
Diameter (mm)	0.55	-
Aspect ratio (-)	65	67
Tensile strength (MPa)	1345	586
Modulus of elasticity (GPa)	210	-
Number of fibers per kg	14500	44950

Three cylinders of 150 mm x 300 mm were cast per series to evaluate the compressive strength. These specimens were cast in three layers; each of them was compacted with a vibration table during 25 seconds. After 24 hours the specimens were unmolded and stored in a curing room at 23°C and 95% of relative humidity for 28 days until the performance of the tests. Besides, six cylinders of 150 mm x 150 mm were cast for each series. Notice that the 150 mm x 150 mm specimens were cut into disks to obtain the specimens for the Luong tests at 21 days of age.

3.2. Material properties

Table 3 presents the results of the fresh- and hardened-state characterization of the mixes. The properties of fresh concrete were evaluated through consistence tests, density tests and entrapped air tests according to the standards ASTM C143 [16], ASTM C138 [17] and ASTM C231 [18], respectively. The hardened-state properties were assessed through compression tests following the standard ASTM C39 [19]. For that, three cylinders of 150 mm x 300 mm were cast per series. Notice that The fresh-state properties of the mixes correspond to typical values for conventional concrete.

Table 3. Fresh- and hardened-state properties of the mixes.

Properties		**Average**			
		SF40	**SF60**	**PF5**	**PF7**
Fresh-state	Slump (cm)	8.0	7.7	7.9	8.0
	Density (kg/m^3)	2255	2247	2260	2250
	Entrapped air (%)	1.5	1.8	1.6	1.7
Hardened-state	Compressive strength (MPa)	40	41	41	41

The influence of the addition of fibers to the fresh-state properties is detected in the density and the entrapped air. The former decreases as the fiber content increases due to the higher porosity of the matrix, whereas the second decreases. The slump for the mixes remains constant or decreases slightly with the incorporation of higher contents of fibers. However, the compressive strength is not significantly affected by the fiber content, as expected.

3.3. Variables of the study

Several variables are evaluated in the study in order to determine their influence in the results, namely the height of the specimen, the diameter of the notch (or the thickness of the external concrete crown that remains outside the perimeter of the notch), the type of fiber and the fiber content. Figure 2 summarizes the variables of the study and the values considered in each case.

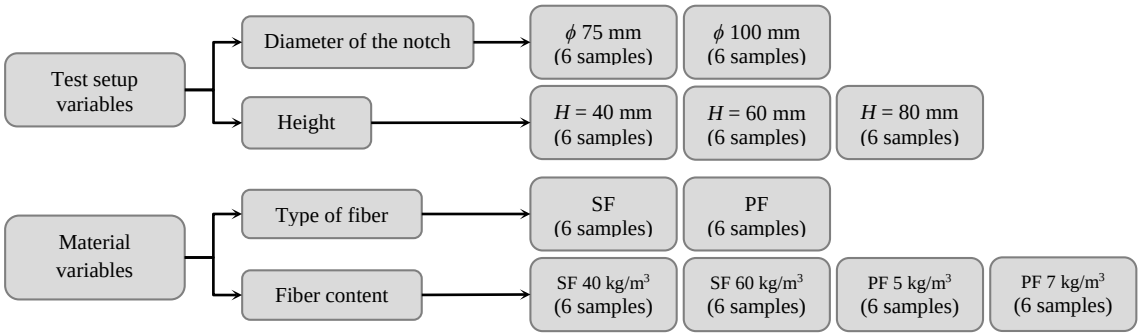

Figure 2. Variables of the study.

The dimension of the notch is determined by the diameter of the drills, which are 75 mm and 100 mm. The diameter of the notch affects the confinement provided by the external crown and the size of the resistant area. The height of the specimens is another variable that affects the shear resistant area. In this case, the values of 40 mm, 60 mm and 80 mm were adopted. The original height proposed by

Luong [15] is 40 mm; however, the length of the fibers available in the market may be larger. For this reason, the other two values were also considered in the study. From the values studied, two are selected for the analysis of the material variables (one for the diameter and one for the height) and remain constant for the subsequent analyses.

Two types of fibers (one steel fiber and one macro-synthetic fiber) were selected in the experimental program. In addition, two fiber contents were considered for each case: 40 kg/m^3 and 60 kg/m^3 for the SF and 5 kg/m^3 and 7 kg/m^3 for the PF. The notation used to designate the specimens starts with the type of fiber, followed by the fiber content, the height and, finally, the diameter of the notch. For example, a specimen reinforced with 40 kg/m^3 of steel fibers, a height of 80 mm and an external crown of 23.5 mm will be referred to as SF40_80_23.5.

3.4. Test setup

A MTS servo-hydraulic load frame with displacement control was used to perform the test. The displacement rate was set to 0.1 mm/min according to previous studies that indicate that high values may lead to an unsuitable control of the test and unreliable results [20]. The same study revealed that a concentrated load distribution close to the notch generates almost a vertical failure plane and, therefore, a more ideal shear failure. For that reason, the loads were applied in a concentrated distribution by means of metallic load rings that do not deform during the test. According to this, the load was applied as indicated in Figure 3a. Besides the load, the axial displacement was registered during the test with three LVDT sensors placed vertically around the specimens and separated 120° one from the other (see Figure 3b). Moreover, the circumferential displacement was also measured by means of a circumferential extensometer located at mid-height of the specimen.

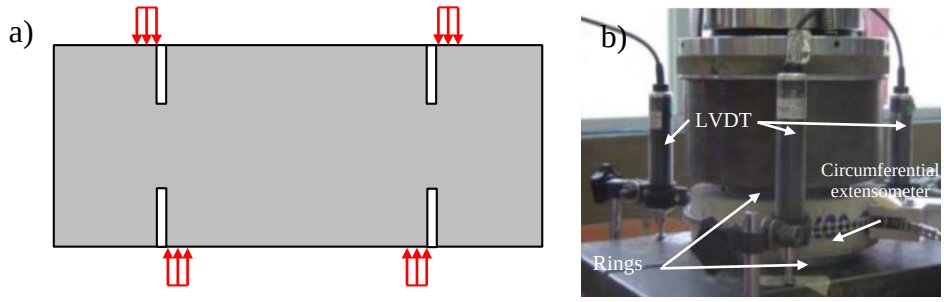

Figure 3. a) Load distribution in the Luong test, b) Luong test setup.

4. ANALYSIS OF THE RESULTS

4.1. Influence of the test setup variables

The influence of the test setup variables in the results of the Luong test are evaluated through the average shear stress-displacement curves of the specimens SF40. Notice that the curves for all specimens are presented together with the average for each case studied. Figure 4a shows the curves of specimens SF40 with different diameters of the notch (75 mm and 100 mm) and the same height (60 mm). Figure 4b presents the curves for specimens SF40 with heights of 40 mm, 60 mm and 80 mm. In this case, the diameter of the notch remains 100 mm for all specimens. Prior to the analysis of the influence of the test setup variables, a general overview of the shear stress-displacement curves yielded by the test is provided. The curves exhibit a linear-elastic behavior until the shear strength of the concrete is reached, as previously introduced while describing the failure mechanism. After the cracking, the specimens present an increase in the stress-bearing capacity due to the combined effect of the aggregate interlock and the fibers. The results of Figure 4 show that the Luong test setup allows reaching relatively large values of displacements. This is a remarkable finding since it means that the test is compatible with the assessment of shear in FRC. Furthermore, despite the variations detected in the post-cracking response, the control of the test is more stable.

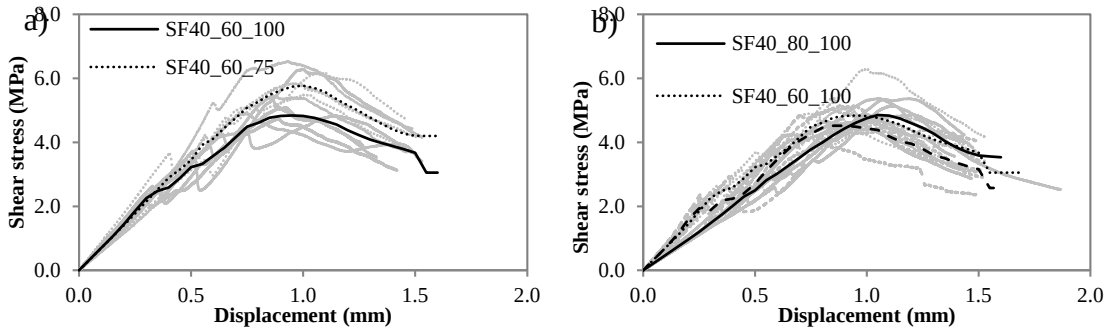

Figure 4. Shear stress-displacement curves for SF40: influence of a) the diameter of the notch and b) the height

The values of load at the moment of cracking obtained from the test indicate that the average shear strength of the specimens with a diameter of the notch of 100 mm and 75 mm are 2.8 MPa and 3.9 MPa, respectively. This represents a shear strength 39.3% higher in the case of the latter. This phenomenon may be attributed to the stronger confinement provided during the linear-elastic stage by the thicker external crown of the specimens with 75 mm of diameter. Figure 4a shows that this tendency continues in the post-cracking stage. In order to analyze the post-cracking behavior, the absorbed energy is estimated as the area below the load-displacement curve. Notice that in order to compare the different specimens, the values of absorbed energy are divided into the failure surface area, thus resulting in a specific absorbed energy (J/m^2). Table 4 presents the values obtained for different displacements.

Table 4. Average absorbed energy for specimens SF40_60_100 and SF40_60_75.

Displacement	Specific absorbed energy (J/m^2)	
	SF40_60_100	**SF40_60_75**
0.5 mm	4.3	4.5
1.0 mm	22.0	24.1
1.5 mm	45.0	49.3

The results show that the specimens with a diameter of the notch of 75 mm present an absorbed energy 4.7%, 9.5% and 9.6% higher than the ones with a notch of 100 mm for displacements of 0.5 mm, 1.0 mm and 1.5 mm, respectively. Again these results may be attributed to the stronger confinement of the external crown in the case of the former. In this regard, a comment should be made on the influence of fiber orientation in the results and, in particular, the wall-effect (a preferential orientation of the fibers along the surface of the formwork, in other words, parallel to the wall). The influence of this phenomenon in the results of the Luong test will depend on the proximity of the failure surface to the area of influence of the wall-effect (near the edges of the specimen). Consequently, the specimens with a notch of 100 mm will be more influenced by the wall-effect than the specimens with a notch of 75 mm.

According to the results in Figure 4b, the average shear strength for the specimens with heights of 40 mm, 60 mm and 80 mm are 2.1 MPa, 2.8 MPa and 2.8 MPa, respectively. These values reveal that increasing the height of the specimen (either to 60 mm or to 80 mm), the shear strength increases 33.3%. Such observation may be related with the ratio between the height characterized and the length of the fibers. As this ratio reduces, the number of fibers crossing the cracked section tends to reduce, thus limiting their overall contribution to the shear behavior. The analysis of the post-cracking stage is conducted through the average specific absorbed energy. For that, the values estimated for displacements of 0.5 mm, 1.0 mm and 1.5 mm are presented in Table 5. The results reveal that the influence of the height of the specimen is not so clear as in the case of the diameter of the notch. In this case, the increase in the height does not lead to higher values of specific absorbed energy for small values of displacement (see values for 0.5 mm and 1.0 mm). This confirms the tendency observed in Figure 4b, in which the increment of height only leads to increases bearing capacity for displacement larger than 1.0 mm. These results and the tendency in Figure 4b, suggests that influence

might reduce or even disappear for a certain size of the specimen. However, increasing the height of the specimens may lead to a different failure mechanism from ideal shear, more influenced by a bending effect.

Table 5. Average absorbed energy for specimens SF40_40_100, SF40_60_100 and SF40_80_100.

Displacement	Specific absorbed energy (J/m^2)		
	SF40_40_100	**SF40_60_100**	**SF40_80_100**
0.5 mm	6.2	4.3	3.1
1.0 mm	24.8	22.0	18.5
1.5 mm	44.6	45.0	41.3

For subsequent analyses, the diameter of the notch 75 mm is selected despite the smaller failure surface in order to avoid the influence of the wall-effect on the results. Furthermore, the height of 60 mm is also selected in order to save material and perform more tests. Notice that the height of 40 mm is discarded given that the length of some of the fibers is over this value (see Table 2).

4.2. Influence of the type and amount of fibers

Two material variables are studied in this section: the type of fiber and the fiber content. Figure 5 presents the shear stress-displacement curves for mixes SF60 and PF7 as well as the resulting average curves for each mix. The curves reveal that after cracking the mix with the highest content of polymeric fiber shows a more pronounced reduction of the load in comparison with the mix with the highest content of steel fiber. This may be attributed to the lower elastic modulus of polymeric fiber, which require bigger displacement in order to start bridging the crack. After this first drop, as fibers become active, the stress resisted increases. Again, this increase is considerably bigger for mixes with steel fiber due to their higher bridging capacity in comparison with plastic fibers. Furthermore, the curves show a significant difference in the stress-bearing capacity between SF60 and PF7.

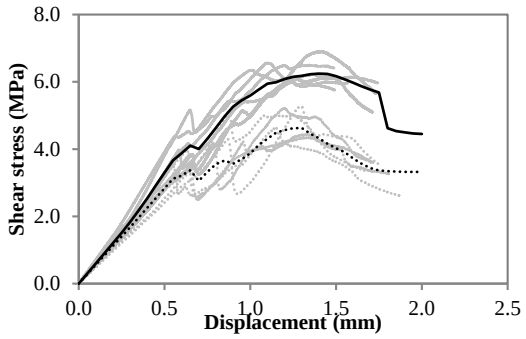

Figure 5. Influence of the type of fiber: load-displacement curves for specimens SF60 and PF7.

The results are confirmed by the values of specific absorbed energy presented in Table 6 for the specimens for SF60 and PF7 (as well as SF40 and PF5 for subsequent analyses), indicating a better performance of the mix SF60. The latter presents values 9.3% and 23.1% higher than PF7 for displacements of 1.0 mm and 1.5 mm, respectively. These results are consistent with the findings by other authors [21-25] regarding the influence of the type of fiber in the tensile post-cracking response of FRC. This suggests that the Luong test is sensible to the variations on the type of fiber.

Figure 6 presents the shear stress-displacement curves of the mixes SF40, SF60, PF5 and PF7 for the analysis of the influence of the fiber content in the results of the Luong test. The curves in Figure 6a reveals an interesting phenomenon for the mixes with SF. Notice that, despite the addition of 20 kg/m^3 of fibers, the specimens with the lowest amount of fibers show stress-bearing capacity up to a displacement of 1.1 mm (see Figure 6a). In fact, the average specific absorbed energy (see Table 6)

for displacements of 0.5 mm, 1.0 mm and 1.5 mm is 95.5% 25.0% and 3.0% higher for SF40 than for SF60. These results may be due to a non-favorable distribution of a higher number of fibers inside the matrix. The average shear stress-displacement curves in **Figure 6a** also show that this tendency changes for advanced values of the displacements, thus indicating that the influence of the fiber content for the mixes with SF is only detected for larger displacements. Therefore, the displacement reached during the test should be larger than 1.5 mm.

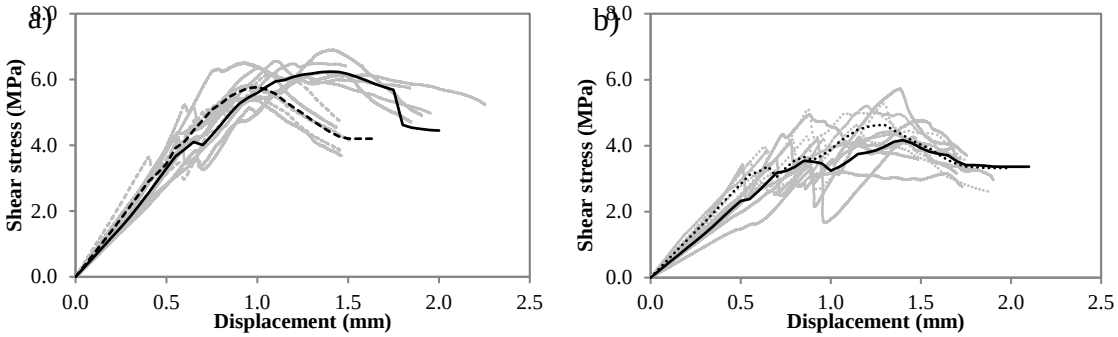

Figure 6. Influence of the fiber content: load-displacement curves for specimens with: a) SF and b) PF.

Figure 6b shows the curves for mixes PF5 and PF7. Due to the noticeable variations observed, particularly for PF5, the analysis is also performed through the average specific absorbed energy presented in Table 6. According to these values, the addition of 2 kg/m^3 of plastic fibers increases the absorbed energy in 78.6%, 29.8%, 19.5% for displacements of 0.5 mm, 1.0 mm and 1.5 mm, respectively. All results confirm that the Luong test is sensible to the fiber content and type.

Table 6. Average absorbed energy for mixes SF40, SF60, PF5 and PF7.

Displacement	Specific absorbed energy (J/m^2)			
	SF40	**SF60**	**PF5**	**PF7**
0.5 mm	4.3	2.2	1.4	2.5
1.0 mm	22.0	17.6	12.4	16.1
1.5 mm	45.0	43.7	29.7	35.5

5. ANALYSIS OF THE SCATTER

Previous sections have evaluated the compatibility and suitability of the Luong test to characterize shear in FRC, however a characterization test must be also reliable. Therefore, analysing the scatter of the results provided by the Luong test is essential in order to be applied for characterization. Figure 7 presents the coefficients of variation (CV) of the values of specific absorbed energy.

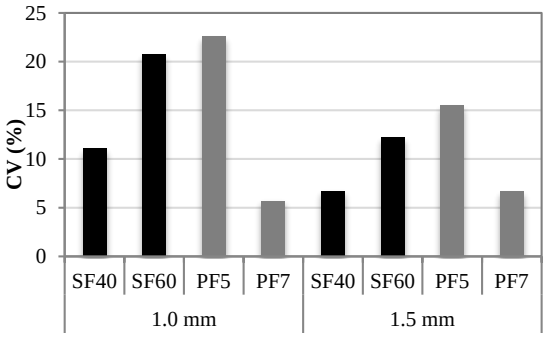

Figure 7. Scatter of the absorbed energy estimated for different values of displacement.

The results are in line with other studies that report the lowest scatter for mixes with macro-synthetic fibers and higher contents due to the larger number of fibers in the concrete matrix [18]. In terms of the steel fibers, no clear trend is detected regarding the fiber content. Besides, Figure 7 reveals other interesting findings. Notice that the *CV* of most specimens remains below 15% and the average value of all specimens is 12.7%. This is relatively low value considering the intrinsic scatter of the material [26] and the high coefficients of variation reported in the literature [27, 28]. Therefore, considering the large scatter associated to FRC, the values of CV obtained in the experimental program are acceptable for the purpose of the test.

6. CONCLUSIONS

The study focuses on the proposal of a simple method for the assessment of the residual shear response of FRC. The Luong test originally proposed to evaluate shear in rocks and plain concrete is selected and adapted for FRC. The results of the experimental program indicate that the Luong test may be a suitable test for characterization of FRC. The main conclusions are presented below:

- The Luong test meets the requirements to be applied for the characterization of FRC given that the setup allows large displacements.
- The control of the test is stable and reliable despite the variations observed in the post-cracking stage. Considering these variations, the evaluating the results may be performed through the specific absorbed energy.
- The Luong test is capable of detecting the influence of the setup variables as the height of the specimen and the diameter of the notch, which affect the size of the fracture surface.
- The variations in the results due to the type of fiber and fiber content are also captured by the test, thus showing that the Luong test is sensitive to the material variables. The analysis also reveals that displacements larger than 1.5 mm should be reached during the test in order to capture the influence of the material variables.
- The analysis of the scatter reveals that the Luong test exhibits relatively low values of the coefficient of variation, being the average value of 12.7% a reference for this test.

ACKNOWLEDGMENTS

The experimental program was conducted in the Laboratory of Structures and Materials of the Institute of Engineering of the UNAM. The authors acknowledge the Institute of Engineering of the UNAM and the International Partnership Fund of the Institute of Engineering of the UNAM for the support in the Partnership Projects of 2014. Likewise, the authors would like to thank the companies Euclid (in particular to Alma Reyes and Víctor Sánchez), BASF (Jorge Esqueda) and Bekaert (Carlos Frutos) for their support in the performance of the experimental program. The authors also acknowledge the collaboration of the postgraduate students Gabriela Zárate and Carlos Ruelas.

REFERENCES

[1] Balázs, G.L. (2010). A historical review of shear. In: *fib Bulletin 57: Shear and punching shear in RC and FRC elements* (pp.1-13). International Federation for Structural Concrete, Lausanne.

[2] Casanova, P., Rossi, P. and Schaller, I. (1997). Can Steel Fibers Replace Transverse Reinforcements in Reinforced Concrete Beams? *ACI Materials Journal*, 94(5), 341-354.

[3] Minelli, F. & Plizzari, G.A. (2013). On the Effectiveness of Steel Fibers as Shear Reinforcement. *ACI Structural Journal*, 110(3), 379-389.

[4] RILEM TC162-TDF (2003). Test and design methods for steel fibre reinforced concrete - σ–e design method-final recommendation. *Materials and Structures*, 36(8), 560–567.

[5] CNR. CNR-DT 204/2006 (2006). *Guide for the design and construction of fiber-reinforced concrete structures*. Italian National Research Council, Rome.

[6] CPH (2008). *Instrucción del Hormigón Estructural EHE-08*, Comisión Permanente del Hormigón, Ministerio de Fomento, Madrid (in Spanish).

[7] fib. (2010). *Model Code for Concrete Structures 2010*. International Federation for Structural Concrete, Lausanne.

[8] AFGC (2013). *Ultra High performance Fibre-Reinforced Concretes. Recommendations*, Association Française de Génie Civil, Paris.

[9] Baby, F., Billo, J., Renaud, J.C., Massotte, C., Marchand, P. and Toutlemonde, F. (2012). Ultimate shear strength of ultra-high fibre-reinforced concrete beams. Proceedings of HIPERMAT 2012, Kassel, p. 484-492.

[10] Van de Loock, L. (1987). Influence of steel fibres on the shear transfer in cracks. In: *Proc. Int. Symposium on Fibre Reinforced Concrete*, Madras.

[11] Balaguru, P. & Dipsia, M.G. (1993). Properties of fiber reinforced high-strength semi-lightweight concrete. *ACI Materials Journal*, 90(5), 399-405.

[12] Valle, M. & Büyüköztürk, O. (1993). Behaviour of fiber reinforced high-strength concrete under direct shear. *ACI Materials Journal*, 90(2), 122-133.

[13] Khaloo, A.R. & Kim, N. (1997). Influence of concrete and fiber characteristics on behavior of steel fiber reinforced concrete under direct shear. *ACI Materials Journal*, 94(6), 592-601.

[14] Echegaray-Oviedo, J., Navarro-Gregori, J., Cuenca, E., Serna, P. (2013). Upgrading the push-off test to study the mechanisms of shear transfer in FRC elements. In: *Proc. VIII Int. Conf. on Fracture Mechanics of Concrete and Concrete Structures (FramCoS-8*) (pp.1-10), J.G.M. Van Mier, G.Ruiz, C. Andrade, R.C. Yu and X.X. Zhang (Eds.), Toledo.

[15] Luong, M.P. (1990). Tensile and shear strengths of concrete and rock. E*ngineering Fracture Mechanics*, 35(1-3), 127-135.

[16] ASTM Standard C143-15. (2015). *Standard Test Method for Slump of Hydraulic-Cement Concrete*. ASTM International, West Conshohocken, PA.

[17] ASTM Standard C138-14. (2014). *Standard Test Method for Density (Unity Weight), Yield and Air Content (Gravimetric) of Concrete*. ASTM International, West Conshohocken, PA.

[18] ASTM Standard C231-14. (2014). *Standard Test Method for Air Content of Freshly Mixed Concrete by the Pressure Method*. ASTM International, West Conshohocken, PA.

[19] ASTM Standard C39 / C39M-05. (2005). *Standard Test Method for Compressive Strength of Cylindrical Concrete Specimens*. ASTM International, West Conshohocken, PA.

[20] Mateo Santana, R.A. (2013). *Caracterización a cortante de hormigón proyectado*. Master Thesis, Universitat Politècnica de Catalunya-BarcelonaTech, Barcelona (in Spanish).

[21] Buratti, N., Mazzotti, C. & Savoia, M. (2011). Post-cracking behaviour of steel and macro-synthetic fibre-reinforced concretes. *Construction and Building Materials*, 25(5), 2713-2722.

[22] Pujadas, P., Blanco, A., de la Fuente, A. & Aguado A. (2012). Cracking behavior of FRC slabs with traditional reinforcement. *Materials and Structures*, 45(5), 707-725.

[23] Blanco, A., Pujadas, P., de la Fuente, A., Cavalaro, S.H.P. & Aguado, A. (2013). Application of constitutive models in European codes to RC–FRC. *Construction and Building Materials*, 40, 246-259.

[24] Blanco, A., Pujadas, P., de la Fuente, A., Cavalaro, S. & Aguado, A. (2014). Constitutive model for fibre reinforced concrete based on the Barcelona test. *Cement and Concrete Composites*, 53, 327-340.

[25] Aire, C., Carmona, S., Aguado, A., & Molins, C. (2015). Double-Punch Test of Fiber-Reinforced Concrete: Effect of Specimen Origin and Size. *ACI Materials Journal*, 112(2), 199-208.

[26] Cavalaro, S.H.P. & Aguado, A. (2015). Intrinsic scatter of FRC: an alternative philosophy to estimate characteristic values. *Materials and Structures*, 48(11), 3537-3555.

[27] Parmentier, B., De Grove, E., Vandewalle, L. & Van Rickstal, F. (2008). Dispersion of the mechanical properties of FRC investigated by different bending tests. In: *Proc. Int. fib Symposium Tailor Made Concrete Structures* (pp. 507-512). Amsterdam.

[28] Molins, C., Aguado, A. and Saludes, S. Double Punch Test to control the energy dissipation in tension of FRC (Barcelona test), Materials and Structures, 2009, 42(4): 415-425.